Agronomy Research **24**(S2), xxx–ccc, 2026
https://doi.org/10.15159/AR.26.061

Spectral behavior of Macaúba palms (*Acrocomia aculeata*) under different lighting conditions and phenological stages

L.S. Santana[1,*], C.L.S. Surmani[1], L.G. Maciel dos Santos[1], M.D.S. Lopes[1] J.M. da Silva[1], A.B. Evaristo[1], G. Rossi[2] and G. Bambi[2]

[1]Institute of Agricultural Sciences (ICA) - Federal University from Jequitinhonha and Mucuri's Valleys (UFVJM) Campus Unaí, Av. Universitária, n°1000 - Unaí, MG, Brasil
[2]Department of Agricultural, Food, Environmental, and Forestry Sciences and Technologies (DAGRI) - University of Firenze (UNIFI), Via San Bonaventura, 13-50145 Florence, Italy
[*]Correspondence: santana.santos@ufvjm.edu.br

Received: January 19th, 2026; Accepted: March 16th, 2026; Published: August 21st, 2026

Abstract. Climate change events highlighted concerns about renewable energy consumption. The Macaúba palm (*Acrocomia aculeata*) stands out as a palm with high potential for energy production. However, it is still in the domestication phase as an agricultural crop. Thus, integrating technologies such as remote sensing to monitor plant characteristics can contribute to understanding this crop's development. In this context, the study aimed to evaluate the spectral behavior of Macaúba (*Acrocomia aculeata*) under various lighting conditions and at different phenological stages. Multispectral images were obtained using a Multispectral Remotely Piloted Aircraft (RPA), with flights conducted at 8:00 AM, 12:00 PM, and 4:00 PM, and during two seasonal periods (February and June 2025). The aim was to analyze the effects of solar variation and plant development on reflectance and spectral indices. The results showed a strong influence of illumination on the spectral response, with an 80% reduction in reflectance under shade, with the red band being the most sensitive. Multitemporal analysis revealed marked decreases in the TCARI (-83.7%), OSAVI2 (-80.8%), and TCARI/OSAVI (-15.9%) indices, accompanied by a decrease in photosynthetic pigments and the onset of leaf senescence during the dry season. Conversely, the NDRE (+10.1%) and CIgreen (+24.7%) indices increased, reflecting maintenance of photosynthetic activity and the emergence of new leaves. NDVI remained stable, indicating the conservation of canopy structure. Multispectral RPAs' potential for phenological and physiological monitoring of tropical palms, emphasizing the importance of temporal and geometric standardization of acquisitions to ensure radiometric consistency. Integrating spectral data with solar parameters is an effective strategy to enhance the sustainable management of Macaúba palms.

Key words: remote sensing, precision agriculture, renewable energy, photogrammetry.

INTRODUCTION

The Cerrado is the second-largest biome in Brazil and Latin America, occupying approximately 22% of the national territory and exceeding 2 million km² (Kuhlmann & Ribeiro, 2021). Recognized as one of the 34 biodiversity hotspots on the planet, it harbors one of the world's richest savannas, with more than 11,000 cataloged native plant species (Caldeira & Parré, 2020). Its environmental heterogeneity, resulting from the interactions among climate, soil, relief, and land use, is expressed in the diversity of vegetation formations, ranging from forest to savanna and grassland physiognomies (Bolfe et al., 2020; Oliveira et al., 2020).

In this context, among the numerous native plant species of the Cerrado, the macaúba (*Acrocomia aculeata*) stands out, a palm tree of great ecological and economic importance, belonging to the Arecaceae family and the Acrocomia genus (Colombo et al., 2018). This species is characterized by its medium to tall size, reaching more than 15 meters in height, and by its high resistance to the climatic conditions of the biome (Duque et al., 2025). The macaúba has been used in the restoration of degraded areas and in the recovery of ecosystems, in addition to having fruits with a high oil content, of interest to the food, cosmetic and, above all, energy sectors, as a raw material to produce biofuels (Fávaro & Rocha, 2022). Phenologically, macaúba presents high intra- and inter-plant variability in reproductive traits and fruit characteristics, indicating heterogeneous developmental patterns among individuals and environments (Ciconini et al., 2013).

The growing demand for renewable energy sources and the diversification of agricultural production have driven macaúba cultivation in different regions of Brazil, mainly in Northwest Minas Gerais, where the species has become established as a sustainable alternative with high productive potential (Silveira et al., 2023). Cultivation systems range from experimental plots to commercial plantations, with cultivated areas varying from small research units to larger production fields depending on management level and production objectives. In addition to its economic importance, macaúba plays a fundamental role in maintaining biodiversity, microclimatic balance, and soil protection (Sant'ana, 2023). Its dense, wide canopy provides shading, altering the distribution of incident solar radiation and, consequently, affecting the spectral response observed by optical sensors (Avelino et al., 2023).

Monitoring plant development and physiological condition has become more accessible and accurate with advances in precision agriculture and remote sensing (Sishodia et al., 2020). The use of Remotely Piloted Aircraft (RPAs) equipped with multispectral cameras enables high-resolution, high-temporal data acquisition, enabling detailed analyses of vegetative vigor, chlorophyll content, and plant nutritional status (Costa et al., 2024). Among the most widely used techniques, photogrammetry stands out, enabling the generation of orthomosaics and digital elevation models from images captured at multiple angles, with an accuracy of a few centimeters (Lavor, 2022).

In dense canopy species, such as macaúba, environmental factors, including variations in light and shading, significantly influence vegetation reflectance and the interpretation of spectral indices derived from images, which can lead to discrepancies in the estimation of biophysical parameters and compromise the spectral recognition of targets (Centeno & Pacheco, 2011). In addition, the phenological stage directly

influences the spectral response, as pigment content (chlorophyll, carotenoids) and leaf structure vary throughout the reproductive cycle (Jiang et al., 2025). In this sense, understanding the variation in macaúba's spectral response across different lighting conditions and phenological stages is essential to improve mapping and remote monitoring methodologies. The integration of spectral data obtained by UAVs enables quantitative and reproducible development, contributing to the selection of more productive and adapted genotypes and to the rational choice of crops.

Therefore, the present study aims to analyze in an integrated way the spectral behavior of macaúba (*Acrocomia aculeata*) under different lighting conditions and phenological stages. It seeks to identify the main differences in spectral response between shaded and illuminated regions and between plant development phases, using spectral indices derived from multispectral images acquired by UAVs.

MATERIALS AND METHODS

Study area

The study area is in a macaúba (*Acrocomia aculeata*) plantation covering 18,500 m², situated on the Santa Paula Experimental Farm (FESP), adjacent to the Campus of the Federal University of the Jequitinhonha and Mucuri Valleys (UFVJM), in the municipality of Unaí, state of Minas Gerais - MG (Fig. 1). The experimental area comprises the coordinates between the meridians (8180810 and 8180975 m S) and parallels (296670 and 296780 m W), inserted in the UTM 23S projection zone, with geodetic reference in the SIRGAS 2000 system.

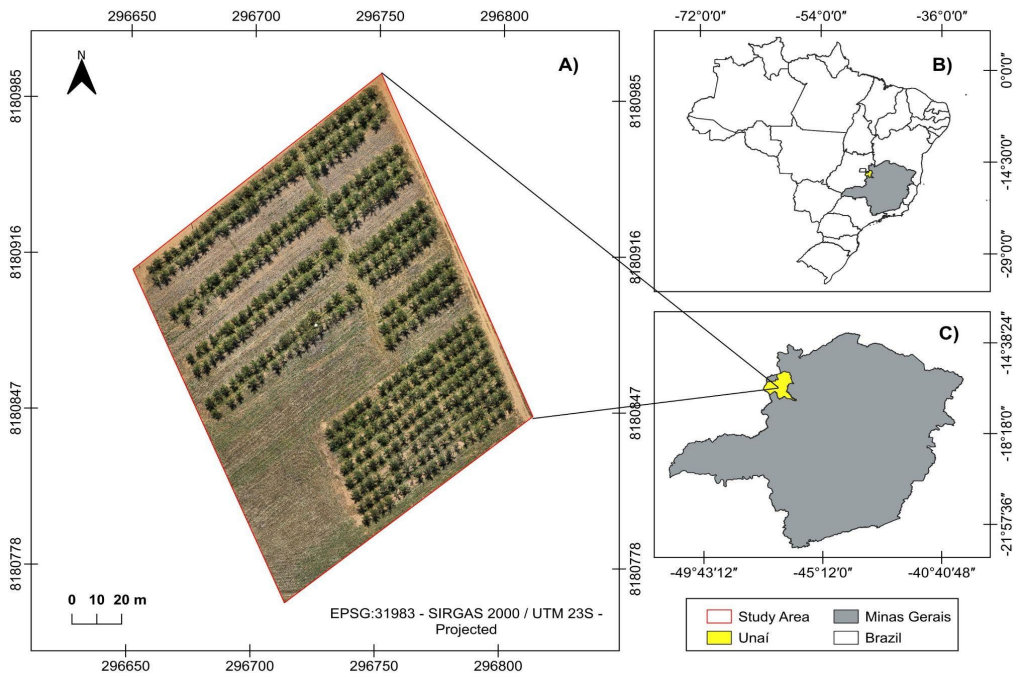

Figure 1. Location of the study area.

The region's climate is classified as Aw, according to the Köppen climate classification, characterized by hot and rainy summers and dry winters, with an average annual temperature of approximately 23 °C and an average yearly rainfall of about 1,322 mm (Silva et al., 2017). The predominant soil in the area is the typical Dystrophic Red Latosol, with a very clayey texture and kaolinitic mineralogy, occurring in flat relief, under the sub-deciduous tropical Cerrado phase (Naime et al., 2014).

Flight parameters and image acquisition

The DJI Mavic 3 Enterprise Multispectral Remotely Piloted Aircraft (Fig. 2, A) was used, equipped with an RGB camera (20 MP) and a multispectral sensor with four 5 MP CMOS sensors (Green - 560 ± 16 nm, Red - 650 ± 16 nm, RedEdge - 730 ± 16 nm, and NIR - 860 ± 26 nm; 3.3 µm pixel). The lens has a focal length of 25 mm, an aperture of f/2.0 and a field of view of 73.91°. The system operates with a maximum speed of 21 m s^{-1}, a shutter speed of up to 1/2000 s, a minimum interval of 0.7 s and a flight time of 43 minutes, with GNSS RTK (Fig. 2, B) for centimeter-level positioning.

Three flights were conducted on June 28, 2025 (8:00 AM, 12:00 PM, and 4:00 PM) to evaluate lighting conditions and minimize shading. Each flight lasted approximately 15 minutes, obtaining 25 shaded and 25 sunny sample points per time slot (total: 150 points). The operational parameters were a speed of 2.6 m s^{-1}, frontal/lateral overlap of 80%/70%, altitude of 30 m, and GSD of 1.38 cm $pixel^{-1}$, resulting in ±400 images per flight. Radiometric calibrations were performed before each mission using a standard reflectance panel (Fig. 2, C), ensuring correction of digital numbers (DN). An additional flight, conducted on February 9, 2025, at 12:00 PM, followed the same temporal parameters and lighting conditions as the previous flight.

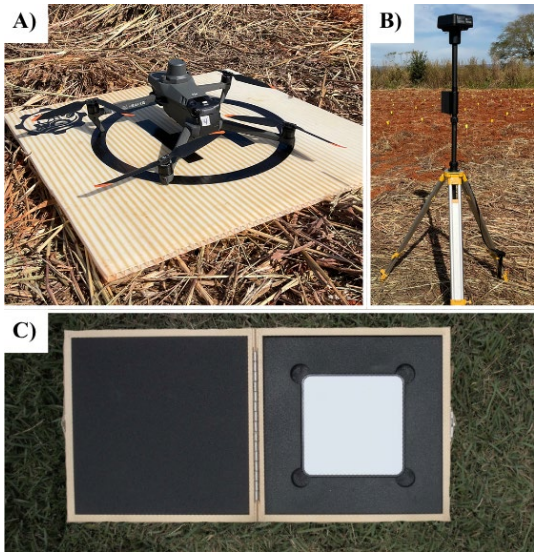

Figure 2. Equipment used: (A) DJI Mavic 3 Enterprise Multispectral, (B) GNSS RTK, and (C) standard reflectance panel.

RGB image processing was performed using Agisoft Photoscan software, resulting in high precision orthomosaics. Before this step, photographs were manually selected, removing duplicates, blurry images, or images with capture flaws to ensure the quality of the material. Images captured at 8:00 AM, 12:00 PM, and 4:00 PM were processed, allowing analysis under different lighting conditions. During processing, the software identifies homologous points, aligns the images, and generates the dense point cloud, the basis for orthorectification and final mosaicking, ensuring geometric and radiometric fidelity.

Pix4D was used exclusively to process the 12:00 PM multispectral images, intended to produce reflectance maps of the Red Edge, NIR, Green, and Red bands captured by the Mavic 3 Enterprise Multispectral. Although it follows a similar workflow to Photoscan, Pix4D offers specific spectral-processing features, enabling greater radiometric control and reflectance calibration. The integration of both software programs enabled more flexible preprocessing and results better suited to the data's spectral characteristics.

Obtaining the Digital Number (DN) and calibrated reflectance

Orthomosaics were imported into QGIS (LTR) 3.40.12 'Bratislava' for spatial analysis. Shapefile point layers representing shaded and sunny areas were created (Fig. 3). The 'Sample Raster Values' tool was used to extract the average Digital Number (DN) values. The conversion of DN to calibrated reflectance was done via an R script, using the "dplyr" package, according to the linear relationship:

$$\rho = a.DN + b \quad (1)$$

where ρ = reflectance (dimensionless); DN = digital value; a and b = calibration coefficients (gain and offset). Average coefficients were applied: $a = 0.0032$ and $b = 0.02$ (red); $a = 0.0028$ and $b = 0.02$ (green); $a = 0.0025$ and $b = 0.02$ (blue). The script generated the columns Reflect_R, Reflect_G, and Reflect_B, with values between 0 and 1, exported as a .csv file.

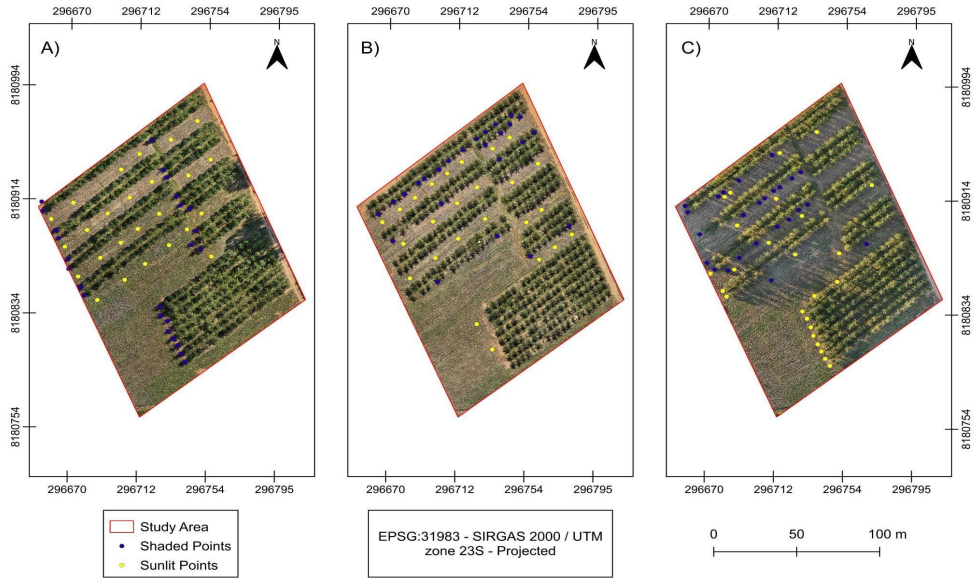

Figure 3. Distribution of sample points in shaded and lighted areas at different times of day: (A) 8am, (B) 12pm and (C) 4pm.

Solar azimuth and altitude calculations were performed using the UTM coordinates of the points, converted to latitude and longitude (SIRGAS 2000, zone 23S). The 'suncalc' package in R was used to determine the solar position (azimuth and altitude, in degrees) at 08:00, 12:00 and 16:00 on 06/28/2025 and at 12:00 on 02/09/2025.

Calculation and analysis of vegetation indices

Multispectral images were used to calculate the NDVI, NDRE, CIgreen, CIred_edge, GNDVI, RENDVI, MCARI, TCARI, OSAVI, and TCARI/OSAVI indices using an R script with the 'terra' and 'sf' packages. Thirty-eight individual plants at the flowering and fruiting stages were analyzed and sampled during flights on February 9 and June 28, 2025. Although macaúba can exhibit overlapping reproductive phases, seasonal patterns are evident in the Cerrado, where flowering is more frequent in the rainy season and fruit development progresses toward the dry season. Thus, the selected dates represented distinct phenological conditions rather than strictly isolated stages. For each plant, spectral index values were extracted directly from the pixels, generating .csv tables and GeoTIFF (.tif) rasters.

The data were subjected to descriptive statistical analysis, including means, standard deviations, and percentage changes between periods, allowing quantification of spectral changes associated with phenological development. This approach allowed quantification of spectral variation associated with morphophysiological modifications in plants, providing a basis for discussion of the patterns observed between the flowering and fruiting stages.

RESULTS AND DISCUSSION

Spectral variation under different lighting conditions

Table 1 presents the average DN and reflectance values for the red, green, and blue bands under shade conditions. It can be observed that the reflectance values were low in all spectral ranges, varying from 0.0680 to 0.3015 in the red band, 0.0648 to 0.2664 in the green band, and 0.0550 to 0.2450 in the blue band. This reduction in reflectance in shaded environments indicates diffuse radiation predominance and the lower contribution of direct radiation, which limits reflected energy fraction detected by the sensors, as observed by de Souza et al. (2021), who noted significant diurnal variations in agricultural canopies reflectance as a function of lighting geometry, with minimum values close to the period of maximum solar altitude due to the reduction in contrast between illuminated and shaded areas.

Table 1. Average values of DN and reflectance under shaded conditions

Time	Red		Green		Blue	
(h)	DN	Reflectance	DN	Reflectance	DN	Reflectance
8:00	27	0.1120	28	0.0984	27	0.0960
12:00	15	0.0680	16	0.0648	14	0.0550
16:00	85	0.3015	88	0.2664	90	0.2450

In Table 2, under direct light conditions, reflectance values increased significantly, ranging from 0.4968 to 0.5509 in the red band, 0.3700 to 0.4288 in the green band, and 0.2700 to 0.2925in the blue band. This increase reflects the direct irradiance effect on the spectral response, reducing diffuse scattering and intensifying reflected radiation. A similar situation was reported

Table 2. Average DN and reflectance values under direct light conditions

Time	Red		Green		Blue	
(h)	DN	Reflectance	DN	Reflectance	DN	Reflectance
8:00	156	0.5192	146	0.4288	109	0.2925
12:00	149	0.4968	125	0.3700	100	0.2700
16:00	156	0.5509	117	0.4032	90	0.2770

by Jafarbiglu & Pourreza (2023), who observed an increase of more than 50% in canopies' reflectance of different crops under higher irradiance, and by Lu et al. (2025), who associated this increase with an improvement in the signal-to-noise ratio and a reduction in geometric shadow effects. These authors also emphasize that angular correction and the use of reflectance indices, such as NIRv and FCVI, contribute to greater consistency in estimating primary productivity across varying illumination conditions.

The comparison between the two conditions shows that the solar angle is a determining factor in reflectance variation. Under shade, the spectral response is modulated by the canopy structure and diffuse radiation fraction, while under direct light, specular reflections and higher signal intensity predominate. Ma et al. (2021) and Jafarbiglu & Pourreza (2023) also found that changes in the solar zenith angle (SZA) and observation geometry significantly affect vegetation indices and the estimation of biophysical parameters.

The red band showed reflectance values 10%–21% higher than those of the green and blue bands, indicating greater sensitivity to irradiance variations. This more intense response is related to chlorophyll absorption and lower multiple scattering in this spectral range, as described by Lunagaria & Patel (2017), who highlighted a more pronounced spectral anisotropy in the red than at shorter wavelengths. The relationship between red reflectance, fluorescence, and primary productivity was also evidenced by Ma et al. (2021) and Lu et al. (2025), who associated diurnal patterns of spectral variation with changes in plant photosynthetic activity. Thus, the results of this study reinforce the notion that lighting conditions are determining factors in reflectance interpretation and in standardizing airborne spectral measurements throughout the day.

Table 3. presents the calculated values of solar azimuth and altitude at different times of day, highlighting the variations in the apparent position of the Sun and its direct influence on surface illumination. The solar altitude increases throughout the day, reaching a maximum near midday. At the same time, the azimuth varies continuously from east to west, a typical behavior of the daily solar displacement. These dynamic influences radiation incidence and, consequently, the shadow and direct light conditions observed in Tables 1 and 2, confirming the relationship between solar geometry and the recorded spectral differences.

Table 3. Variation of solar azimuth and altitude throughout the day

Variable	Time (h)		
	08:00	12:00	16:00
Azimuth	58.64°	4.02°	303.94°
Solar altitude	16.91°	50.19°	21.45°

Moriya et al. (2018) analyzed angular variation in the reflectance of sugarcane canopies. They observed that changes in viewing angle and solar position alter the reflectance intensity, even though the spectral shape remains similar, characterizing the vegetation's anisotropic behavior and reinforcing that differences in solar angle can also significantly influence the radiometric response. In turn, Jenčo (2025) emphasized that the precise determination of the solar incidence angle is crucial for understanding the amount of energy reflected and absorbed by a surface. The author highlights that the geometric calculation of the solar angle, combined with the definition of extreme incidence times, allows us to understand the temporal variation of radiation and its impact on the spectral response. Thus, the values obtained in this study for solar azimuth and altitude reinforce the importance of geometric illumination characterization in reflectance spectral interpretation of data acquired by airborne sensors.

Spectral variation between phenological stages

Phenological classification was performed through direct field observation immediately before each flight, in which each plant was assigned to its predominant stage (spathe, flowering, fruiting, or abortion) and later linked to the corresponding UAV spectral data. Spectral analysis of macaúba (*Acrocomia aculeata*) plants in Unaí–MG revealed significant modifications between the spathe, flowering, fruiting, and abortion stages. Spectral indices derived from UAV multispectral images showed variations consistent with phenological transitions and seasonal conditions in the Minas Gerais Cerrado, a behavior like that reported by Medeiros et al. (2022) in the Caatinga biome. Table 4 presents the descriptive statistics of spectral indices obtained during the two flights (1) in 09 February 2025 and (2) 28 June 2025, corresponding to the end of the rainy season and the beginning of the dry season.

Table 4. Descriptive statistics of spectral indices obtained in two flights over Macaúba palm trees

Flight	Statistic	Mean	SD	Median	Minimum	Maximum	SE	CV (%)
1	NDVI	0.806	0.052	0.816	0.62	0.874	0.008	6.48
	NDRE	0.308	0.04	0.304	0.229	0.392	0.006	12.85
	CIgreen	5238	1103	5018	2954	7994	0.179	21.06
	TCARI	0.033	0.01	0.031	0.014	0.056	0.002	31.51
	OSAVI2	0.037	0.006	0.038	0.024	0.05	0.001	16.89
	TCARI/OSAVI	0.875	0.178	0.914	0.435	1229	0.029	20.3
2	NDVI	0.808	0.045	0.045	0.635	0.883	0.007	5.56
	NDRE	0.339	0.046	0.046	0.248	0.458	0.008	13.66
	Cigreen	6532	1855	1855	3851	12669	0.301	28.4
	TCARI	0.005	0.002	0.002	0.001	0.013	0	38.22
	OSAVI2	0.007	0.002	0.002	0.004	0.011	0	21.67
	TCARI/Osavi	0.736	0.171	0.171	0.319	1208	0.028	23.24

*SD: Standard Deviation and SE: Standard Error.

For example, individual plants classified in the fruiting stage showed localized reductions in TCARI and OSAVI values in canopy sectors associated with older leaves, while newly emitted leaves displayed higher NDRE values, a pattern that reflects the broader trends observed in Table 4. Between the two evaluated periods (February and June 2025), the TCARI (-83.7%), OSAVI2 (-80.8%), and TCARI/OSAVI (-15.9%) indices showed marked reductions, while NDRE (+10.1%) and CIgreen (+24.7%) showed significant increases. NDVI remained practically stable (+0.3%), suggesting that the overall canopy structure remained constant. Variations in average magnitude (~24%) indicate a significant spectral reorganization across phenological stages.

The reduction in pigment indices (TCARI, OSAVI2, and TCARI/OSAVI) reflects lower absorption in red, associated with decreased chlorophyll in part of the canopy and localized leaf senescence. Similar patterns were observed by Baluja et al. (2012), who related variations in TCARI/OSAVI to water availability and physiological stress in grapevines. This behavior suggests that the transition from spathe to initial fruiting in macaúba coincides with physiological adjustments at the onset of the dry season, typical of seasonal tropical environments.

The increases observed in the NDRE and CIgreen indices indicate maintenance of photosynthetic activity and the emission of new leaves. NDRE is recognized for its sensitivity to nitrogen and chlorophyll content in tropical palms (Hariadi et al., 2024). In

contrast, CIgreen shows a strong correlation with chlorophyll content in the canopies of perennial species (Balan et al., 2025). These results suggest that, even with reduced pigmentation in older leaves, the canopy parts retained physiologically active leaves during fruiting.

Lighting conditions also influenced spectral variations. In the first flight (February), the solar azimuth ranged from 98° to 264°, with solar altitude between 27° and 84°, resulting in greater shadow heterogeneity. Gao et al. (2024) highlight that indices based on visible bands, such as TCARI, are more sensitive to angular variations. In contrast, red-edge index, such as NDRE, are more stable under these conditions. This explains the consistency of the red-edge indices between the two flights.

In addition, the seasonal differences between the collection periods reflect the typical behavior of tropical perennial species. In a study of oil palm in Malaysia, Li et al. (2025) observed that multitemporal variations in reflectance are associated with palm age and alternation between wet and dry periods, indicating that spectral indices are effective at detecting subtle phenological changes. In the present study, macaúba palms exhibited a similar pattern, with expressive spectral reorganization, even without significant alteration in the canopy structure. These findings suggest that multispectral imaging may help distinguish macaúba from other palm species in mixed environments due to differences in canopy structure, pigment dynamics, and phenology. However, further comparative studies are required to confirm this potential under operational conditions.

CONCLUSIONS

The spectral response of macaúba (*Acrocomia aculeata*) varied strongly with lighting conditions and phenological stage. The intensity and angle of solar radiation directly affected reflectance values, with a greater response to direct light and a significant reduction under shade, highlighting the need for temporal and geometric standardization in multispectral data acquisition and the importance of shading in radiometric calibration.

Variations in the TCARI, OSAVI2, and TCARI/OSAVI indices indicated a reduction in the content of photosynthetic pigments associated with leaf senescence. At the same time, NDRE and CIgreen showed maintenance of physiological activity and the emergence of new leaves. Thus, the integration of spectral data obtained by Remotely Piloted Aircraft (RPAs) proved to be an effective tool for multitemporal monitoring of macaúba, allowing the identification of subtle phenological transitions and improving remote sensing methodologies for Cerrado perennial species. These advances also support future research aimed at optimizing crop monitoring, genotype selection, and site-specific management, contributing to more sustainable production systems and to the strategic use of macaúba as a renewable resource for bioenergy and bioproduct chains.

ACKNOWLEDGEMENTS. Special thanks to the NEMA research group for their assistance with field data collection and equipment operation, to the (DAGRI) Department of Agricultural, Food, Environmental, and Forestry Sciences and Technologies UNIFi – Firenze It, Research Support Foundation of the State of Minas Gerais (FAPEMIG: APQ-01151-23) and National Council for Scientific and Technological Development CNPq (MAI&DAI: 401042/2024-3).

REFERENCES

Avelino, N.R., Campos, L.J.M., Aires, D.M., Silva, R.S. da, & Barbosa Evaristo, A. 2022. Shadowing of a bioenergetic species in soybean development: an analysis of the feasibility potential of this integration. *Acta Scientiarum. Agronomy* **45**, e57497. doi: 10.4025/actasciagron.v45i1.57497

Balan, P., Paulose, S.V., Joseph, T. & Devasia, J.M. 2025. Retrieval of Spectral Responses of Rubber Plantations and its Association to Canopy Chlorophyll Content Using Sentinel 2 Data and Field Measurements. *Agricultural Research*. doi: 10.1007/s40003-025-00883-2

Baluja, J., Diago, M.P., Balda, P., Zorer, R., Meggio, F., Morales, F. & Tardaguila, J. 2012. Assessment of vineyard water status variability by thermal and multispectral imagery using an unmanned aerial vehicle (UAV). *Irrigation Science* **30**(6), 511–522. https://doi.org/10.1007/s00271-012-0382-9

Bolfe, E.L., Sano, E.E., Campos, S.K. 2020. *Agricultural dynamics of the Cerrado: analyses and projections*. Brasília: *Embrapa*, 308 pp. (in Portuguese).

Caldeira, C. & Parré, J.L. 2020. Agricultural diversification and rural development in the Cerrado biome. *Revista Americana de Empreendedorismo e Inovação* **2**(1), 344–359 (in Portuguese). https://doi.org/10.33871/26747170.2020.2.1.3356

Centeno, J.A.S. & Pacheco, A.da P. 2011. Shadow classification in orbital and aerial images using a modified co-occurrence matrix. *Boletim de Ciências Geodésicas* **17**(1), 75–92 (in Portuguese). https://doi.org/10.1590/S1982-21702011000100005

Ciconini, G., Favaro, S.P., Roscoe, R., Miranda, C.H.B., Tapeti, C.F., Miyahira, M.A.M., Bearari, L., Galvani, F., Borsato, A.V., Colnago, L.A. & Naka, M.H. 2013. Biometry and oil contents of Acrocomia aculeata fruits from the Cerrados and Pantanal biomes in Mato Grosso do Sul, Brazil. *Industrial Crops and Products* **45**, 208–214. doi: 10.1016/j.indcrop.2012.12.008

Colombo, C.A., Berton, L.H.C., Diaz, B.G. & Ferrari, R.A. 2018. Macauba: a promising tropical palm for the production of vegetable oil. *OCL* **25**(1), D108.doi:10.1051/ocl/2017053

Costa, R.P., Fernandes, L.L.D.A., Muta, L.F., Isatto, E.L. & Costa, D.B. 2024. 3D building modeling generated by photogrammetry using Unmanned Aerial Vehicles (UAVs). (English abstr.). *Ambiente Construído* **24**, e131377 (in Portuguese). doi:10.1590/s1678-86212024000100739

Duque, T.S., Barroso, G.M., Borges, C.E., Mendes, D.S., da Silva, R.S., Evaristo, A.B. & dos Santos, J.B. 2025. Current and future development of Acrocomia aculeata focused on biofuel potential and climate change challenges. *Scientific Reports* **15**(1), 8120. https://doi.org/10.1038/s41598-025-92681-7

Favaro, S.P. & Rocha, J.D. 2022. The new macauba production chain for bioproducts and decarbonization. Brasília, DF: *Embrapa Agroenergia*, 31 pp. (in Portuguese).

Gao, S., Yan, K., Liu, J., Pu, J., Zou, D., Qi, J., Mu, X. & Yan, G. 2024. Assessment of remote-sensed vegetation indices for estimating forest chlorophyll concentration. *Ecological Indicators* **162**, 112001. https://doi.org/10.1016/j.ecolind.2024.112001

Hariadi, B., Sastrohartono, H., Krisdiarto, A.W., Sukarman, S., Sagoro, T.H., Primananda, S., Akbar, A.R.M. & Uktoro, A.I. 2024. The Use of the Normalized Difference Red Edge (NDRE) Vegetation Index from Multispectral Cameras Mounted on Unmanned Aerial Vehicle to Estimate the Nutrient Content in Oil Palm Leaves. *Jurnal Teknik Pertanian Lampung (Journal of Agricultural Engineering)* **13**(4), 1051. doi: 10.23960/jtep-l.v13i4.1051-1063

Jafarbiglu, H. & Pourreza, A. 2023. Impact of sun-view geometry on canopy spectral reflectance variability. ISPRS J. Photogramm. *Remote Sens*. **196**, 270–286. doi:10.1016/j.isprsjprs.2023.01.005

Jenčo, M. 2025. Determination of the Solar Angle of Incidence Using an Equivalent Surface and the Possibility of Applying This Approach in Geosciences and Engineering. *ISPRS International Journal of Geo-Information* **14**(9), 323. https://doi.org/10.3390/ijgi14090323

Jiang, C., Cheng, Y., Li, Y., Peng, L., Dong, G., Lai, N. & Geng, Q. 2025. Phenology-Aware Machine Learning Framework for Chlorophyll Estimation in Cotton Using Hyperspectral Reflectance. *Remote Sensing* **17**(15), 2713. https://doi.org/10.3390/rs17152713

Kuhlmann, M. & Ribeiro, J.F. 2021. *Restoration of native vegetation in the Cerrado biome: questions and answers*. Planaltina, DF: Embrapa Cerrados, 210 pp.

Lavor, Melyssa Sousa de. 2022. *The use of UAV photogrammetry in urban land regularization: the case of Salgueiro – PE.* Trabalho de Conclusão de Curso *(*Bacharelado em Engenharia Civil*)* - Unidade Delmiro Gouveia - Campus do Sertão, Universidade Federal de Alagoas, Delmiro Gouveia, 82 pp. (in Portuguese).

Li, C., Chen, B., Wang, X., Ong-Abdullah, M., Wu, Z., Lan, G., Azmi Tohiran, K., Amit, B., Lai, H., Wang, G., Yun, T. & Kou, W. 2025. Integrating Multi-Temporal Landsat and Sentinel Data for Enhanced Oil Palm Plantation Mapping and Age Estimation in Malaysia. *Remote Sensing* **17**(16), 2908. https://doi.org/10.3390/rs17162908

Lu, X., Yang, P., Arthur, A.M. & van der Tol, C. 2025. Using reflectance to reduce solar angle effects on the scattering of far-red solar-induced chlorophyll fluorescence to better track the diurnal dynamics of gross primary productivity. *Agricultural and Forest Meteorology* **373**, 110794. https://doi.org/10.1016/j.agrformet.2025.110794

Lunagaria, M.M. & Patel, H.R. 2017. Changes in reflectance anisotropy of wheat crop during different phenophases. *International Agrophysics* **31**(2), 203–218. doi: 10.1515/intag-2016-0045

Ma, D., Rehman, T U., Zhang, L., Maki, H., Tuinstra, M.R. & Jin, J. 2021. Modeling of Diurnal Changing Patterns in Airborne Crop Remote Sensing Images. *Remote Sens.* **13**(9). doi:10.3390/rs13091633

Medeiros, R., Andrade, J., Ramos, D., Moura, M., Pérez-Marin, A.M., dos Santos, C.A., ... & Cunha, J. 2022. Remote Sensing Phenology of the Brazilian Caatinga and Its Environmental Drivers. *Remote Sens.* **14**(11). doi:10.3390/rs14112601

Moriya, É.A.S., Imai, N.N. & Tommaselli, A.M.G. 2018. A Study on The Effects of Viewing Angle Variation in Sugarcane Radiometric Measures. *Boletim de Ciências Geodésicas* **24**(1), 85–97. https://doi.org/10.1590/s1982-21702018000100007

Naime, U.J., Motta, P.E.F.da, Silva, D.C.da, Simão, M.L.R., Santos, A.J.R.dos. 2014. *Soils and assessment of the agroforestry potential of the microregions of Paracatu and Unaí - Minas Gerais*. Belo Horizonte: Epamig, 106 pp. (in Portuguese).

Oliveira, M.T. de, Cassol, H.L.G., Ganem, K.A., Dutra, A.C., Prieto, J.D., Arai, E. & Shimabukuro, Y.E. 2020. Mapping the Cerrado Vegetation – A Review of Remote Sensing Initiatives (in Portuguese). *Revista Brasileira de Cartografia* **72**, 1250–1274. https://doi.org/10.14393/rbcv72nespecial50anos-56591

SANT'ANA, Cíntia Tomaz. 2023. *Chemical characterization and in vitro and in vivo functional properties of macaúba (Acrocomia aculeata)*. PhD Thesis (Doutorado em Ciência e Tecnologia de Alimentos) - Universidade Federal de Viçosa, Viçosa. 165 pp. (in Portuguese)

Silva, D.V., Cunha, F.F., Vicente, M.R., Alencar, C.A.B., & Souza, I. P. 2017. Analysis of Precipitation, Climatological Water Balance, and Climate Classification in the Municipality of Unaí-MG. *Braz. Geogr. J.* **8**(1), 68–82.

Silveira, V.A. da, Paula, H.B. de, Francelino, M.R., Filpi, H.E.F.C.M., Kuki, K.N., Zanuncio, J.C. & Imbuzeiro, H.M.A. 2023. Agroclimatic reference for Acrocomia aculeata (Jacq.) Lodd. ex Mart. based on its center of diversity in Minas Gerais, Brazil (in Portuguese). *Ciência Florestal* **33**(4), e64546. https://doi.org/10.5902/1980509864546

Sishodia, R.P., Ray, R.L. & Singh, S.K. 2020. Applications of Remote Sensing in Precision Agriculture: A Review. *Remote Sensing* **12**(19), 3136. https://doi.org/10.3390/rs12193136

Souza, R.M. de, Ortigara, Y.V.B., Gomes, C.E.M., Magalhães, R.R., Fontanini, P.S.P. & Campos, A.T. 2024. Eco-efficiency of self-compacting concrete using sanitary ware waste. *Ambiente Construído* **24** (in Portuguese). doi: 10.1590/s1678-86212024000100739

Wang, C., Su, Y., Wang, J., Wang, T. & Gao, Q. **2022**. UAVSwarm Dataset: An Unmanned Aerial Vehicle Swarm Dataset for Multiple Object Tracking. *Remote Sensing* **14**(11), 2601. https://doi.org/10.3390/rs14112601